BJRS

BRAZILIAN JOURNAL
OF
RADIATION SCIENCES
10-03 (2022) 01-17

Performance based on NEMA NU-4 2008 Standard of CDTN/CNEN's Small Animal PET Scanner

Gontijo, R.M.G.[a,b]; Ferreira A.V.[b]; Silva J.B.[b]; Mamede M.[a,b]

[a] *Department of Anatomy and Imaging, Federal University of Minas Gerais, 30130-100, Belo Horizonte-MG, Brazil*

[b] *Radiopharmaceuticals Research and Production Unit, Center of Nuclear Technology Development, 31270-901, Belo Horizonte-MG, Brazil.*

rgadelha@ufmg.br

ABSTRACT

This study evaluated the general performance of the preclinical PET scanner (LabPET Solo 4, GE) at CDTN/CNEN based on the NEMA NU 4-2008 standard. The parameters included: (i) spatial resolution; (ii) scatter fraction and counts rate performance; (iii) sensitivity and (iv) image quality. The results revealed that the radial spatial resolution ranged from 1.79 mm at the center of the FOV to 2.49 mm at a radial offset of 25 mm, while the tangential resolution ranged from 1.95 mm at the center of the FOV to 3.50 mm at a radial offset of 25 mm and the axial resolution ranged from 1.78 mm at the center of the FOV to 5.42 mm at a radial offset of 25 mm. Iterative image reconstruction improved the radial spatial resolution to 0.93 mm at the center of the FOV. The peak noise equivalent count rate was 37.8 kcps at 85 MBq whereas the peak true count rate was 169.9 kcps at 125 MBq with a count loss of 7.8 % for the maximum rate reached at 103.3 MBq. The peak of sensitivity at the center of axial field-of-view was 5.7 cps.Bq^{-1}. The image roughness was 9.5 %. Spillover rates in air and in water were 0.26 and 0.17 respectively. The recovery coefficients were 0.12 for the 1-mm-diameter rod and 0.91 for the 5-mm-diameter rod. The results demonstrate that the scanner produce satisfactory quality image and is well suited for preclinical molecular imaging research when compared with international literature results that use similar systems.

Keywords: **quality control program; preclinical PET; NEMA NU 4-2008.**

ISSN: 2319-0612
DOI: https://doi.org/10.15392/bjrs.v10i3.2006
Submitted:2022-02-08
Accepted: 2022-06-15

1. INTRODUCTION

Most of molecular imaging research is undertaken in small animals (e.g, preclinical PET scanner imaging) which provide a bridge between *in vitro* studies and human clinical imaging. Thus, PET for small animals can be considered a translational research tool between animal models and human clinical applications [1].

Currently in Brazil, there are six laboratories of preclinical molecular imaging using seven PET systems routinely for the development of new radiopharmaceuticals or in studies of new applications of traditional radiopharmaceuticals [2]. Therefore, a comprehensive evaluation of the performance of these systems is necessary to optimize the obtained images.

The National Electrical Manufactures Association (NEMA) published its NU 4-2008 standards, a consistent set of methodologies for measuring scanner performance parameters for small animal PET imaging [3]. However, according to the literature, there is no Brazilian recommendation or requirement for the execution of a quality assurance program for preclinical imaging centers.

In this context, this work is the first Brazilian study about quality control in preclinical PET [4] scanners in national laboratories and aimed to evaluate the general performance of the preclinical PET scanner (LabPET Solo 4, GE) at CDTN/CNEN based in NEMA NU 4-2008 standardized methods.

2. MATERIALS AND METHODS

The experiments were carried out at CDTN/CNEN in the Molecular Imaging Laboratory (LIM) and with collaboration of the Radiopharmaceutical Research and Production Unit (UPPR), which made the ^{18}F-FDG sources (Radioglic®) available.

In this work were used the LIM/CDTN/CNEN small animal PET scanner and specific phantoms to evaluate counts rate performance and image quality as well as a sealed radioactive source of Sodium-22 to evaluate spatial resolution and sensitivity.

2.1. PET SCANNER

The Triumph^{TM} platform is a preclinical system dedicated for rodents imaging. The subsystem LabPET 4 installed at LIM/CDTN/CNEN consists of a stationary gantry with 1536 detection channels. It employs an Avalanche Photo Diode (APD) detector ring incorporating an assembly of LYSO (Lutetium yttrium oxyorthosilicate – $Lu_{1.9}Y_{0.1}SiO_5$) and LGSO (Lutetium gadolinium oxyorthosilicate – $Lu_{0.4}Gd_{1.6}SiO_5$) scintillators optically coupled one after the other [5].

LabPET 4 images are acquired using a 250-650 keV energy window and 22 ns coincidence timing window. It provides axial field of view (FOV) of 3.7 cm and can operate in a dynamic or static mode. Coincident data are saved in list mode and can be sorted out as sinograms. More details about the LabPET 4 design and architecture are presented elsewhere [6, 7].

2.2. NEMA NU 4-2008 TESTS

2.2.1. SPATIAL RESOLUTION

The spatial resolution test purpose is to characterize the full width at half-maximum amplitude (FWHM) and the full width at tenth-maximum amplitude (FWTM) of the reconstructed image point spread function of a compact radioactive source [3].

The compact source used consists of a ^{22}Na point source with activity of 1.154 MBq (reference date on certificate: 2018/12/01) confined to no more than 0.3mm³, embedded in an acrylic cube of 1cm³ (Eckert & Ziegler Isotope Products).

Data were collected using the point source positioned in scanner's FOV center (Z=0 mm) and one-fourth of the axial FOV (Z=27.75 mm) at the radial offset distances of 0, 5, 10, 15 and 25 mm. Each measured lasted 2 minutes adding up at least of 10^5 prompt counts. The image acquisition and processing to obtain spatial resolution in radial, tangential and axial directions followed strictly the NEMA NU 4–2008 standards.

Image reconstructions were performed using the 2D filtered backprojection (FBP) method with no smoothing. In addition, the spatial resolution was also calculated using iterative reconstruction applying the LIM/CDTN/CNEN standard protocol [MLEM-3D algorithm, 20 iterations and no high-resolution mode] [8]. Data was processed using AMIDE® software. The spatial

resolution (FWHM and FWTM) in all three directions - radial, tangential and axial - were determined by peak analysis of the point source image. Volumetric resolution was calculated from the product of spatial resolution in all orthogonal directions at the center of axial FOV (z=0 mm) and ¼ from the center of axial FOV.

2.2.2. COUNT RATE PERFORMANCE

The purposes of count rate performance test are (i) to measure the relative system sensitivity to scattered radiation and (ii) to measure the effects of system dead-time and the generation of random coincidence events at several levels of source activity [3].

To achieve these purposes, a specially designed scatter phantom (mouse-like) made up of a solid, circular cylinder composed of polymethylmethacrylate (PMMA) was used according to NEMA 4-2008 specifications. The mouse-sized phantom is 70 ± 0.5 mm long and 25 ± 0.5 mm in diameter. A cylindrical hole (3.2 mm diameter) is bored parallel to the central axis at a radial offset of 10 mm for this phantom. At this cylindrical hole, a line source may be inserted, consisting of a clear flexible tube with a radiopharmaceutical fillable section.

The ^{18}F-FDG solution activity into the line source was 202 MBq at the beginning of image acquisition, which lasted 18 hours. To evaluate intrinsic scanner count rate another acquisition during the same time was performed for the mouse phantom without radioactive solution. Data were acquired after placing the phantom at the center of the FOV parallel to the Z-axis of the scanner. Acquisition procedure followed the recommendation of NEMA NU 4-2008 publication [3] while the analysis procedure was adapted by the authors because there is no way to extract the sinogram from acquired images. The acquisition time (18 h) were subdivided into 62 intervals (Frames 1 up to 37 - alternating times of 10 and 60 seconds - and frames 38 up to 62 - alternating times of 1 hour and 10 seconds). After that, the total data time of the measurement was processed using the iterative reconstruction method (MLEM-3D algorithm, 20 iterations and no high-resolution mode).

For all time acquisition, prompt count rate of all coincidences was extracted from reconstruction output file. The noise equivalent count rate (NECR) for each frame of acquisition was calculated as

$$\boldsymbol{NECR} = \frac{\boldsymbol{R_{true}^2}}{\boldsymbol{R_{total} + R_{random}}} \qquad (1)$$

where R_{true} is the true event rate, R_{total} is the total event rate and R_{random} is the random event rate [3].

In addition, count loss rate was measured from the count rate linearity of true coincidence events as a function of activity in the field of view.

2.2.3. Sensitivity

The sensitivity test purpose is to measure the ability of the scanner to convert activity into count rates [3]. Sensitivity is expressed in counts per second, that true coincidence events are detected for a given source strength and branching ratio. Absolute sensitivity is the fraction of positron annihilation events detected as true coincidence events. The source employed to perform the sensitivity test was the same used in the above-described spatial resolution measurements (^{22}Na; 1.154 MBq).

The point source was placed in scanner's FOV axially and transaxially centered. Acquisitions were performed for 2 minutes adding up at least of 10.000 true events each. Total of 21 measurements was performed at positions stepped axially covering the whole scanner's FOV axial. The background true event rate was also measured but in the absence of the radioactive source. All data were analyzed according to NEMA NU 4-2008 publication.

2.2.4. Image Quality

The image quality test purpose is to produce images that simulate those acquired in the whole-body study of a small animal [3]. For this purpose, a specially designed image quality (IQ) phantom made up of polymethylmethacrylate (PMMA) with internal dimensions of 50 length and 30 mm diameter was used (Figure 1).

Figure 1: *(A) IQ Phantom; (B) IQ Phantom Schematic View*

(A)

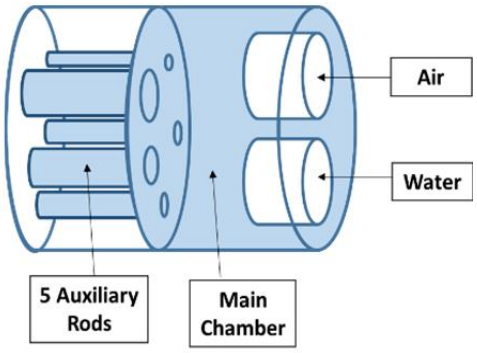

(B)

The IQ phantom was designed by NEMA NU 4/2008 and consists of 3 different regions to analyze distinct characteristics:

(i) Uniformity (%SD of the activity concentration): indicator of the system signal to noise ratio.

(ii) Spillover ratio (SOR) in each (air and water) cold region: indicator of the system scattering correction performance

(iii) Recovery coefficient (RC): indicator of the system spatial resolution

Acquisition and image analysis procedures followed the recommendation of NEMA NU 4-2008 publication methodology (3.7 MBq activity of ^{18}F-FDG at the beginning of acquisition; 20 min acquisition time). PET images were reconstructed following the LIM/CDTN/CNEN standard protocol [8]: MLEM-3D algorithm; 20 iterations; no high-resolution mode; no attenuation or scatter corrections; no post-filtering. PMOD® software was used to perform images post-processing following NEMA NU 4-2008 recommendations.

3. RESULTS AND DISCUSSION

3.1. Spatial Resolution

The measured radial, tangential, and axial spatial resolutions in terms of FWHM and FWTM (mm) at two different axial positions were plotted for both FBP and iterative reconstruction methods. Figures 2 and 3, respectively, show FWHM and FWTM for measurements at the center of the axial FOV.

Figure 2: *Radial, tangential, and axial spatial resolution (FWHM) for the FBP and MLEM reconstruction methods as a function of radial offset of the point source at the center of the axial FOV.*

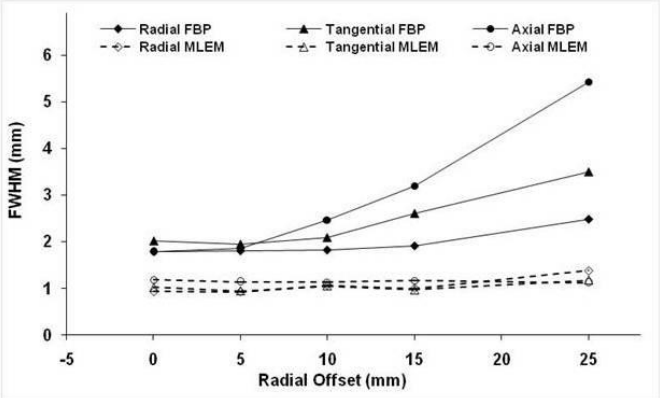

Figure 3: *Radial, tangential, and axial spatial resolution (FWTM) for the FBP and MLEM reconstruction methods as a function of radial offset of the point source at the center of the axial FOV.*

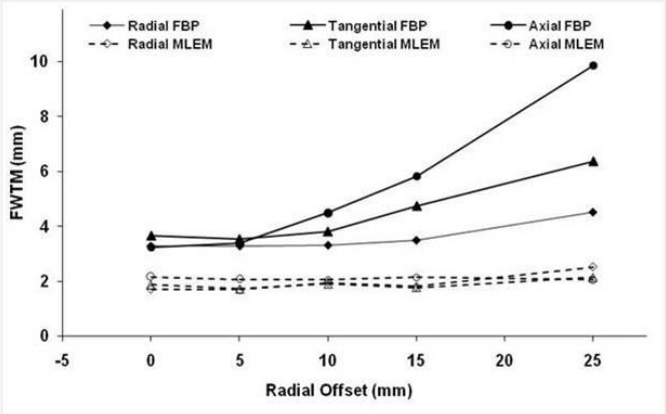

Figures 4 and 5, respectively, show FWHM and FWTM for measurements at ¼ from the center of the axial FOV.

Figure 4: *Radial, tangential, and axial spatial resolution (FWHM) for the FBP and MLEM reconstruction methods as a function of radial offset of the point source at ¼ from the center of axial FOV.*

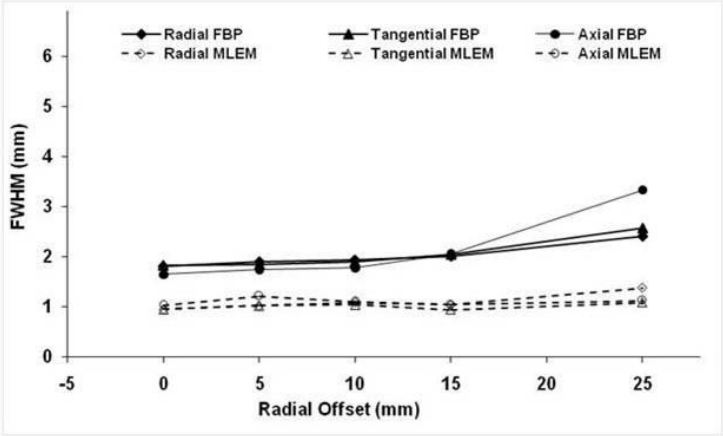

Figure 5: *Radial, tangential, and axial spatial resolution (FWTM) for the FBP and MLEM reconstruction methods as a function of radial offset of the point source at ¼ from the center of axial FOV.*

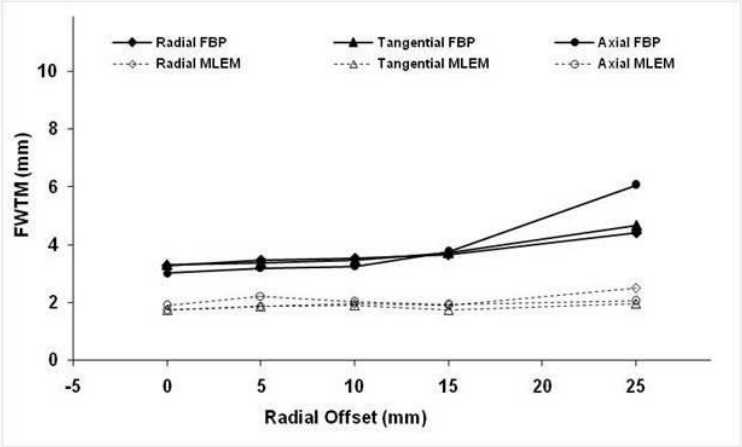

For FBP reconstruction as recommended by the NEMA 4-2008 publication, the FWHM volumetric resolution at the center of axial FOV (z=0 mm) and ¼ from the center of axial FOV (z=0.925 mm) is 6.40 mm^3 and 5.41 mm^3, respectively.

For iterative reconstruction, the FWHM volumetric resolution at the center of axial FOV (z=0 mm) and ¼ from the center of axial FOV (z=0.925 mm) is 1.15 mm^3 and 0.93 mm^3, respectively.

Spatial resolution in terms of FWHM and FWTM was generally better at the ¼ position from the center of axial FOV than at the center, particularly for axial resolution, because of the more oblique lines of response used by the central position than by the ¼ from the center of axial FOV position.

Image reconstructed by analytical method (FBP) presents noise-streaks around the point source and the spatial resolution values varied significantly in all three directions along the transversal FOV in both cases (center of FOV and ¼ of center of FOV). Iterative reconstruction (MLEM), with accurate statistical modeling the image physical data processed by the system, improved substantially the spatial resolution in all three directions. The FWHM values found for iterative reconstruction in the three axes (x and y $\leq$ 1.0 mm and z $\leq$ 1.5 mm) agree with results recommended by manufacturer on its service guide [5].

The iterative algorithms are better, as they try to compensate for physical and/or technological limitations like the scanner geometry as well as positron range.

3.2. Count Rate and Count Losses

Figure 6 presents the count rate performance of the PET scanner for the mouse-sized phantom. The total, true, random, scatter and NEC count rates are plotted against the effective activity into the mouse-sized phantom.

Figure 6: *Count Rate performance as a function of the activity of the line source for mouse-sized phantom.*

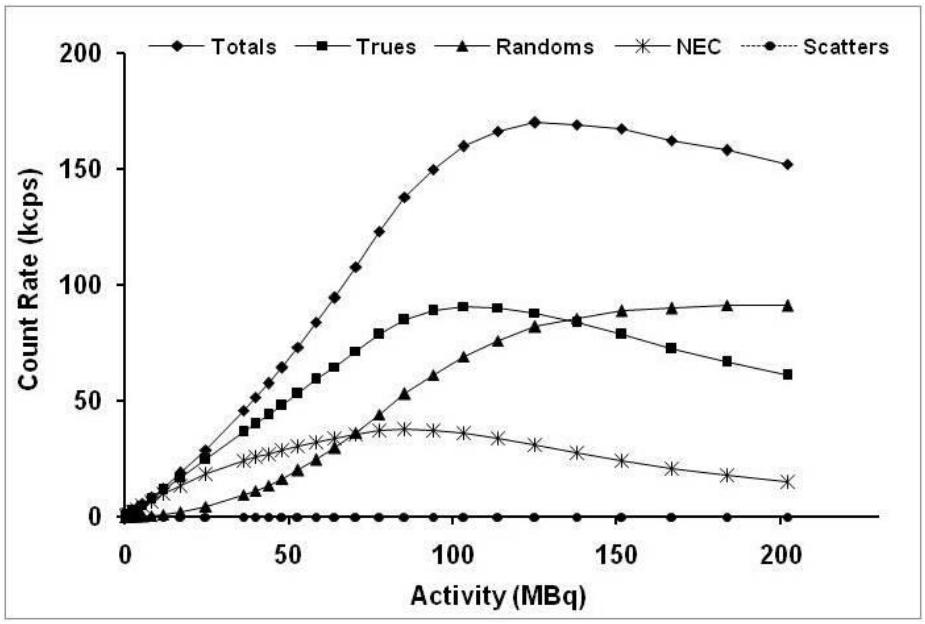

The Figure 6 reveals that the true event count rates increase to around 100 MBq and then decline again. It is also found that the number of true events is substantially greater than the number of random events until around 120 MBq. After that the number of random events overtakes the number of true events. The total event rate consists mainly of true and random events. Scattered coincidence events are always reported as zero because they are not counted by this system. The peak NECR is 37.8 kcps at 85 MBq whereas the peak true count rate is 169.9 kcps at 125 MBq.

In low activities range, the counting rates increase proportionally with the activity. This fact is expected because greater activity results in more disintegrations and therefore more events detected. But at any time, detectors will no longer be able to keep up with the increase in events due to dead time. The profile of count rates performance obtained is very similar with other LabPET scanners [9].

Count loss is represented in Figure 7 and is based on the linearity of the true events count rate as a function of the activity. Count loss of 7.8 % was obtained comparing number of the true events count rate calculated by linear function and the maximum rate reached at 103.3 MBq.

Figure 7: *Count Loss obtained from true events rate as function of the activity*.

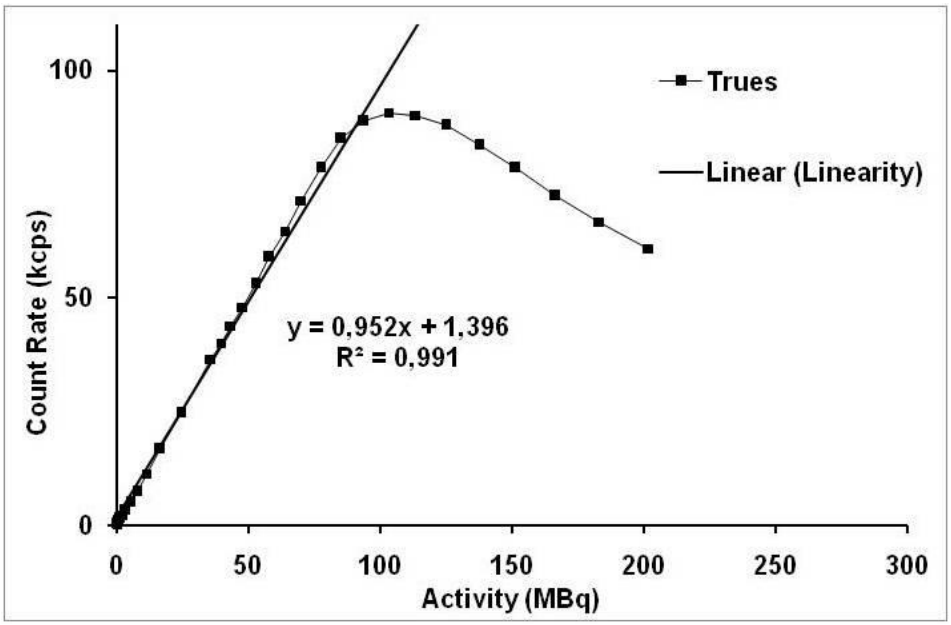

Since most animal studies at LIM/CDTN are performed with up to 20 MBq of activity (eg; mouse whole body with ^{18}F-FDG), count losses (< 10 %) due to dead time or maximum data throughput can be considered negligible in these studies.

3.3. Sensitivity

The peak of sensitivity (S) and absolute sensitivity (SA) at the center of axial FOV were 5.7 cps.Bq^{-1} and 0.63 %, respectively. Figure 8 shows the axial absolute sensitivity (SA) profile along the z-axis of the LabPET Solo 4 scanner of LIM/CDTN/CNEN.

The axial profile of absolute sensitivity revealed higher scanner sensitivity around the center of the FOV (0.63 %) and decreasing sensitivity towards the ends of the FOV, as expected. However, the system peak absolute sensitivity is less than that found in another study (1.33 %) for the LabPET 8 model [10]. This found was expected and can be explained due to number of crystals in each scanner. In LabPET 8 model this number is twice that of LabPET 4 model used in this work.

Figure 8: *The axial absolute sensitivity profile*.

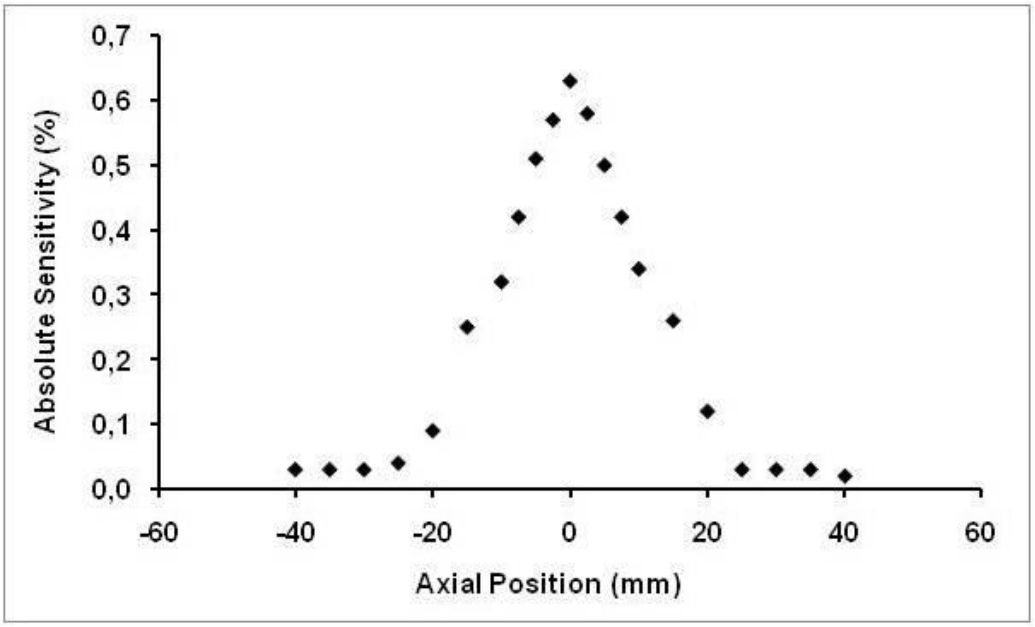

The LabPET platform has three distinct models (named 4, 8 and 12) and different thresholds for the energy window (250-650 or 350-650 keV). However, for LabPET 4 used in this work it was not possible to assess the sensitivity of the system with the threshold (350 – 650 keV) because the range (250 – 650 keV) is on default and cannot be changed. The narrow energy window configuration, although providing lower detection efficiency, would account for less associated noise and would evidence a significant gain for sensitivity, as described in literature [9].

3.4. Image Quality

Representative image of the NEMA NU 4-2008 image quality phantom obtained at LIM/CNEN is shown in Figure 9.

The mean, maximum, minimum and the percentage standard deviation of activity concentration results are presented in Table 1.

Figure 9: *Typical image in (A) axial, (B) coronal and (C) sagittal planes of NEMA NU 4-2008 image quality phantom acquired at LIM/CDTN/CNEN*.

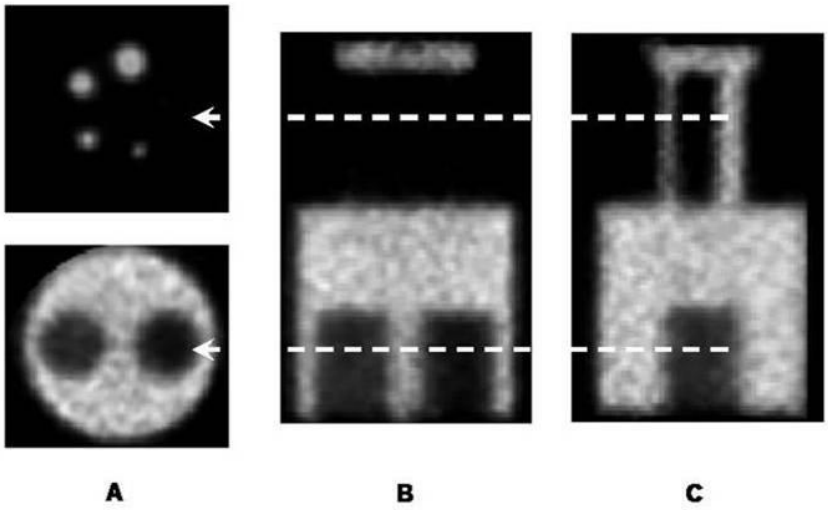

Table 1: Uniformity Test results

Activity Concentration			
Mean (kBq/mL)	**Maximum (kBq/mL)**	**Minimum (kBq/mL)**	**% STD**
184.8	250.1	126.8	9.5

Spillover Ratios (SOR) and the respective percentage standard deviations obtained for the cold chambers (water and air-filled) are reported in Table 2.

Table 2: Spill-over Ratio Test results

Region	SOR	% STD
Water-filled	0.17	18.9
Air-filed	0.26	17.8

Recovery Coefficients (RCs) and respective percentage standard deviations for the five diameters rods are shown in Table 3.

Table 3: Recovery Coefficient Test results

RC	**1 mm**	**2 mm**	**3 mm**	**4 mm**	**5 mm**
	0.12	0.54	0.81	0.90	0.91
% STD	39.3	35.2	33.1	39.0	33.3

The image roughness was like those obtained by Bergeron *et al* (2009) - 9.5 % STD - for a LabPET 4 scanner [11] in contrast to 7.0 % reported for the LabPET 8 scanner [10].

The SOR is an indication of the performance of system for the scatter correction. SOR values obtained for the cold chamber filled with water are compatible with the value reported by Prasad *et al*. (2011) for the model LabPET 8 (Water SOR: 0.20) [10]. However, the SOR values obtained for the cold chamber filled with air (Air SOR: 0.26) are significantly higher than those reported by those authors (Air: 0.11) [11]. This fact may be explained by different characteristics between the PET scanners. The LabPET 4 model used in this work is not able to perform corrections for attenuation and scatter while the upper model LabPET 8 performs both corrections.

The RC values for the five distinct rods varied from 0.12 to 0.91 and is an indication of the spatial resolution of the system. These values are very similar to those previous reported from periodic evaluations for the same LabPET™ scanner used in this work [12] - from 0.11 to 0.89 - and for the LabPET 8 [10] - from 0.13 to 0.96.

4. CONCLUSIONS

The overall performance of the LabPET Solo 4 scanner installed at LIM/CDTN was characterized based on the NEMA NU 04–2008 standards.

The performance measurements reported in this paper are unprecedented in Brazil and follow as closely as possible the standard methodology NEMA for evaluating of PET scanners designed for preclinical use.

In general, the LIM/CDTN small animal PET scanner performance results demonstrate that it produces satisfactory quality image and is well suited for preclinical molecular imaging research when compared with international literature results that use similar systems [5; 9 - 11].

Despite of the satisfactory results and quality images obtained it is essential of routinely carrying out quality control procedures to maintain the reliability and stability of quality parameters of the scanner. The authors group intent to carry out intercomparisons between the preclinical PET scanners of the different Brazilian laboratories. The results of this project will serve as a subsidy for a national standardization of the quality control protocols necessary to harmonize the use of the pre-clinical molecular image in the research field.

ACKNOWLEDGMENT

This work was partially financial supported by CNPq, FAPEMIG, CDTN/CNEN and UFMG.

The authors also thank the staff of the Molecular Imaging Laboratory (LIM) and Radiopharmaceutical Research and Production Unit (UPPR) of CDTN/CNEN.

REFERENCES

[1] YAO R.; LECOMTE R.; CRAWFORD E. Small-Animal PET: What is it, and why do we need it? **Journal of Nuclear Medicine Technology**. Vol. 40 nº3, pp.157-165. 2012.

[2] GONTIJO, R. M. G. **Proposta de Programa de Garantia da Qualidade para Imagem Molecular Pré-Clínica.** 2019. 275 f. Doctoral Thesis (Doutorado em Ciência e Tecnologia das Radiações, Minerais e Materiais) – Centro de Desenvolvimento da Tecnologia Nuclear, Comissão Nacional de Energia Nuclear, Belo Horizonte, In Portuguese, 2019.

[3] NEMA - National Electrical Manufacturers Association. **Performance Measurements of Small Animal Positron Emission Tomographs**. Rosslyn VA; 2008 Standards Publication NU 4-2008.

[4] GONTIJO, R. M. G., FERREIRA, A. V., SILVA, J. B., MAMEDE, M. Quality control of small animal PET scanner: The Brazilian Scenario. **Brazilian Journal of Radiation Sciences**. vol. 08 (2). pp. 1-09. 2020.

[5] GE Healthcare Technologies, 2011. **Triumph Service Guide Technical Publication**. Revision Draft 6, Copyright. Available in: <http://www.gehealthcare.com> 2011.

[6] TETRAULT, M.A. *et al*., 2008. System Architecture of the LabPET Small Animal PET Scanner. IEEE **Transactions on Nuclear Science**. 55(5), 2546-2550.

[7] FONTAINE, R. *et al*. 2009. The hardware and signal processing architecture of LabPETTM, a small animal APD-based digital PET scanner. IEEE **Transactions on Nuclear Science**. 56, 3-9.

[8] GONTIJO, R. M. G., FERREIRA, A. V., SILVA, J. B., MAMEDE, M. Image quality assessment using NEMA NU 4/2008 standards in small animal PET scanner. **Brazilian Journal of Radiation Sciences**. 07(2A). pp. 1-13. 2019.

[9] BERGERON, M. *et al*. Imaging performance of LabPET APD-based digital PET scanners for pre-clinical research. **Physics in medicine and Biology**. 59, 661-678. 2014.

[10] PRASAD, R., RATIB, O., ZAID, H. NEMA NU-04-based Performance Characteristics of the LabPET-8TM Small Animal PET Scanner. **Physics in Medicine and Biology**. 56(20), 6649-6664. 2011.

[11] BERGERON, M. *et al*. Performance Evaluation of the LabPET APD-Based Digital PET Scanner. IEEE **Transactions on Nuclear Science**. 56(1). 2009.

[12] GONTIJO, R.M.G., FERREIRA, A.V., SOUZA, G.C.A., MENDES, B.M., SILVA, J.B., MAMEDE, M. 2020. Image quality evaluation of a small animal PET scanner. **Brazilian Journal of Radiation Sciences**. 8(1), 01-13. 2020.

[13] IAEA - International Atomic Energy Agency (IAEA). Quality Control Guidance for Nuclear Medicine Equipment. **Guidelines of Radiation and Nuclear Safety Authority** – STUK, 2010.

[14] GONTIJO, R. M. G., FERREIRA, A. V., SOUZA, G. C. A., BARBOSA, J. V. C., MAMEDE, M. Current Brazilian Scenario about Quality Assurance in preclinical PET imaging systems. In: **INTERNATIONAL NUCLEAR ATLANTIC CONFERENCE**, 2021 Virtual meeting**.** Annals Brazil, November 29 – December 2, 2021.

[15] OSBORNE, D. R., KUNTNER, C., BERR, S., STOUT, D. Guidance for Efficient Small Animal Imaging Quality Control. **Molecular Imaging and Biology.** 19pp. 485-498. 2016.